Supplementary information

Unprecedented structural variations in trinuclear mixed valence Co(II/III) complexes derived from a Schiff base and its reduced form: Theoretical studies, pnicogen bonding interactions and catecholase-like activities

Alokesh Hazari,[a] Lakshmi Kanta Das,[a] Ramakant M. Kadam,[b] Antonio Bauzá,[c] Antonio Frontera*[c] and Ashutosh Ghosh*[a]

[a]Department of Chemistry, University College of Science, University of Calcutta, 92, A.P.C. Road, Kolkata-700 009, India. E-mail: ghosh_59@yahoo.com

[b]Radiochemistry Division, Bhabha Atomic Research Centre, Trombay, Mumbai 400085, India

[c]Department of Chemistry, Universitat de les IllesBalears, Crta de Valldemossa km 7.5, 07122 Palma de Mallorca, Baleares, Spain. E-mail: toni.frontera@uib.es

Table S1 Crystal data and structure refinement of complexes **1**–**3**

	1	**2**	**3**
Formula	$C_{36}H_{40}Co_3N_{16}O_6$	$C_{34}H_{40}Co_3N_{16}O_8$	$C_{34}H_{40}Co_3N_{16}O_4$
M	969.63	977.61	967.67
Crystal System	Triclinic	Triclinic	Triclinic
Space Group	$P\bar{1}$	$P\bar{1}$	$P\bar{1}$
a/Å	10.290(4)	9.270(5)	14.906(5)
b/Å	18.442(7)	9.533(5)	9.326(5)
c/Å	22.634(9)	12.660(5)	15.164(5)
α/°	71.323(5)	106.395(5)	90.000(5)
β/°	89.960(5)	101.926(5)	92.428(5)
γ/°	83.263(5)	99.741(5)	90.000(5)
V/Å^3	4038(3)	1018.8(9)	2106.1(15)
Z	4	1	2
D_c/g cm^{-3}	1.595	1.593	1.526
μ/mm^{-1}	1.286	1.278	1.232
F (000)	1988.0	501.0	998.0
R(int)	0.063	0.019	0.037
Total Reflections	27114	13270	21543
Unique reflections	13847	5985	7395
$I>2\sigma(I)$	9774	5110	5594
R1[a], wR2[b]	0.1254, 0.3456	0.0318, 0.0922	0.0407, 0.1153
GOF[c] on F^2	1.05	1.05	1.07
R (all)	0.1542	0.0387	0.0578
Temp (K)	296	293	293

[a]$R1 = \sum||F_o| - |F_c||/\sum|F_o|$, [b]$wR2\ (F_o^2) = [\sum[w(F_o^2 - F_c^2)^2/\sum w\ F_o^4]^{½}$ and [c]$GOF = [\sum[w(F_o^2 - F_c^2)^2/(N_{obs} - N_{params})]^{½}$

Table S2 The r.m.s deviations of the complexes **1**–**3**.

Metal centers	R.M.S Deviations (Å)			
	1		**2**	**3**
	1A	**1B**		
Co(2)	0.032	0.035	0.013	0.027
Co(3)	0.057	0.052	---	0.028

Table S3 The ∠N-N-N angles (in °) in azido ligands in the complexes **1**–**3**.

	1A	**1B**	**2**	**3**
N(1)–N(2)–N(3)	174.6(2)	175.4(2)	178.8(2)	178.1(6)
N(10)–N(11)–N(12)	175.0(2)	177.7(2)	---	173.2(2)
N(4)–N(5)–N(6)	177.4(2)	177.0(2)	---	176.4(8)
N(7)–N(8)–N(9)	176.5(2)	175.3(2)	175.3(2)	176.9(8)

Table S4 Hydrogen Bond Interactions in Complex **3**.

D–H···A	D–H(Å)	H···A(Å)	D···A(Å)	∠D–H···A(°)	Symmetry
C(38)–H(38A)–N(12B)	0.970	2.620	3.434(1)	141.00	x,1+y,z
C(17)–H(17B)–N(12A)	0.969	2.632	3.439(2)	140.93	x,-1+y,z
C(20)–H(20B)–N(9)	0.970	2.717	3.400(1)	128.06	x,-1+y,z
C(41)–H(41B)–N(6)	0.970	2.743	3.418(1)	127.17	x,-1+y,z

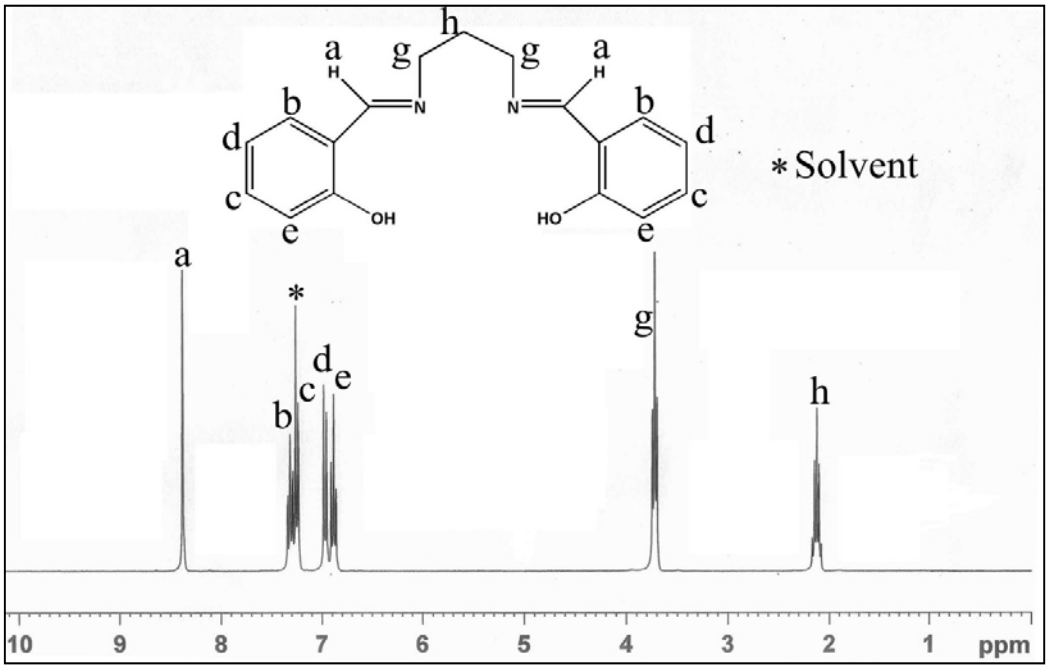

Fig. S1 ^{1}H-NMR spectrum of ligand (H_2L) in $CDCl_3$

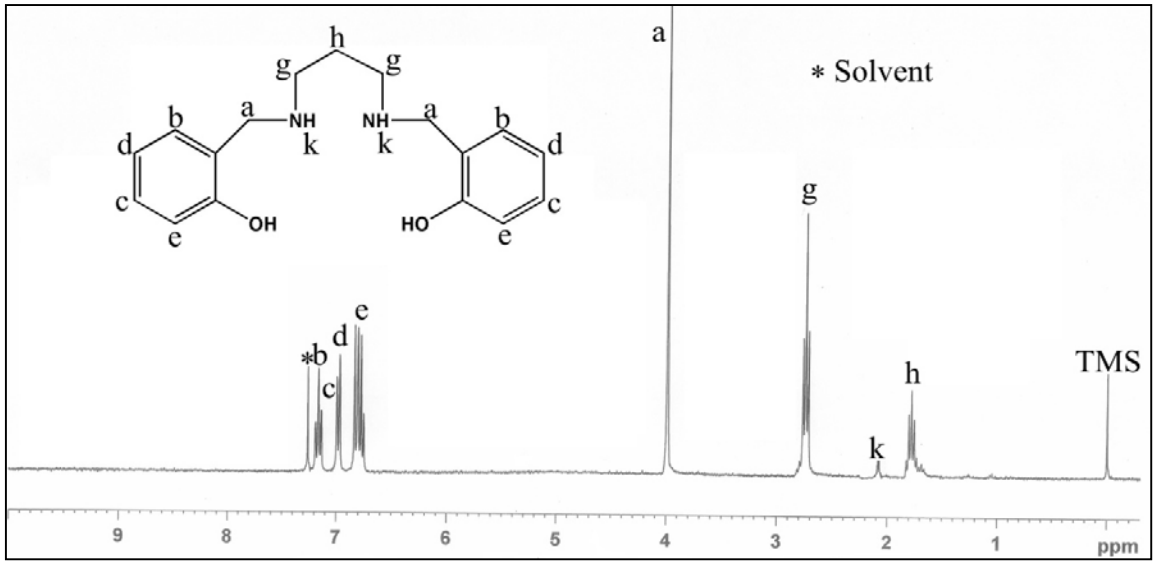

Fig. S2 ^{1}H-NMR spectrum of ligand (H_2L^R) in $CDCl_3$

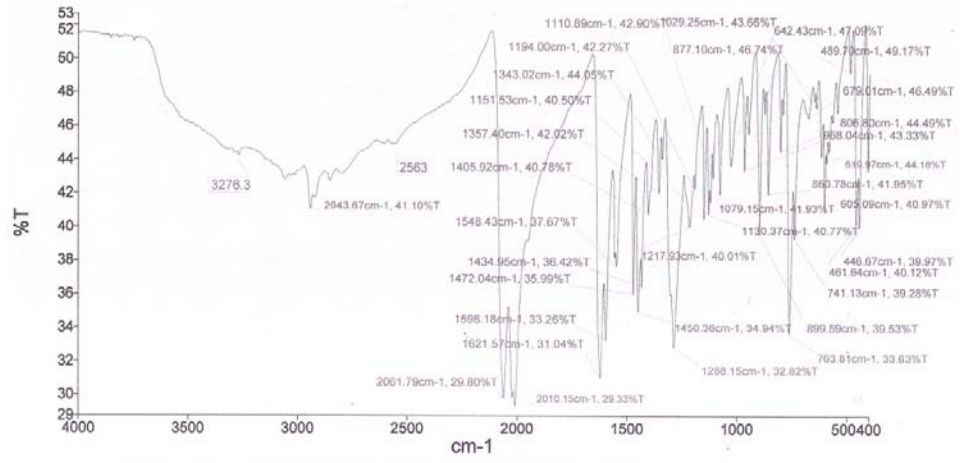

Fig. S3 IR spectrum of complex **1**.

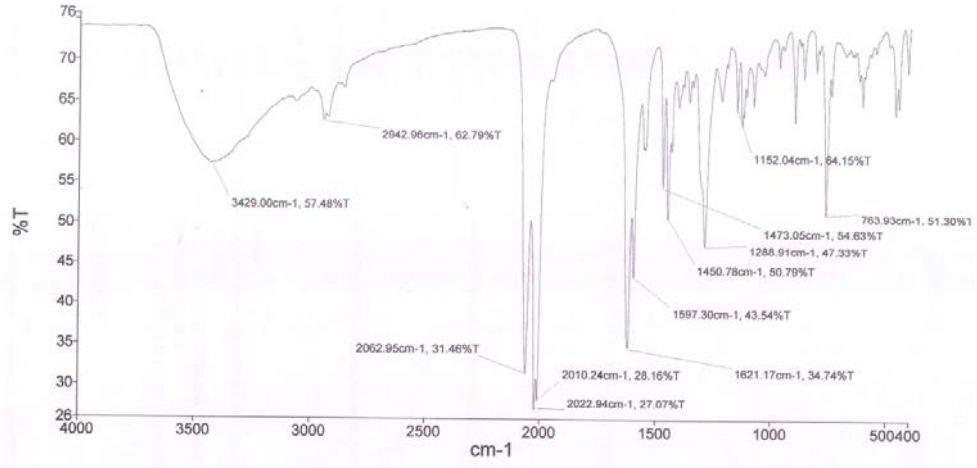

Fig. S4 IR spectrum of complex **2**.

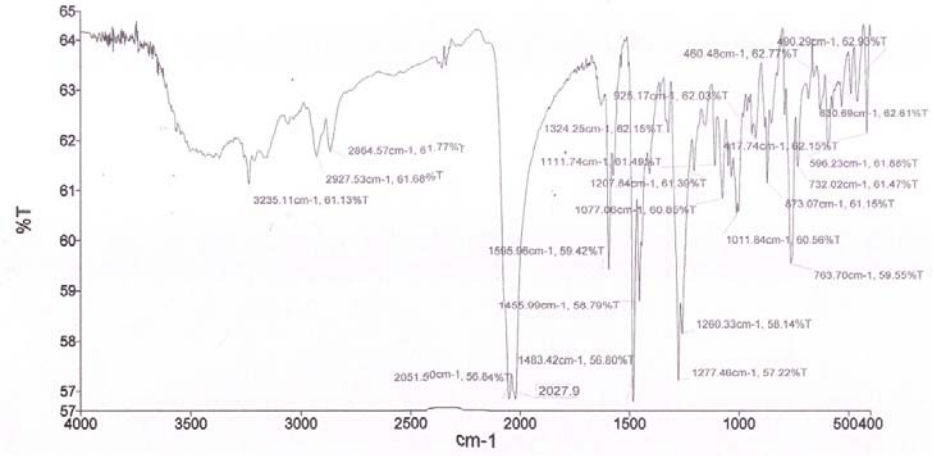

Fig. S5 IR spectrum of complex **3**.

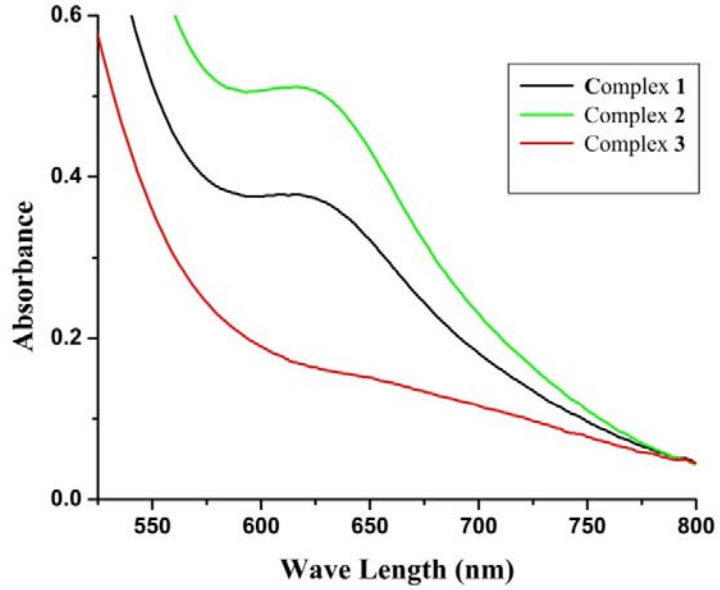

Fig. S6A UV-Vis spectra of trinuclear complexes in acetonitrile solution (d-d transition).

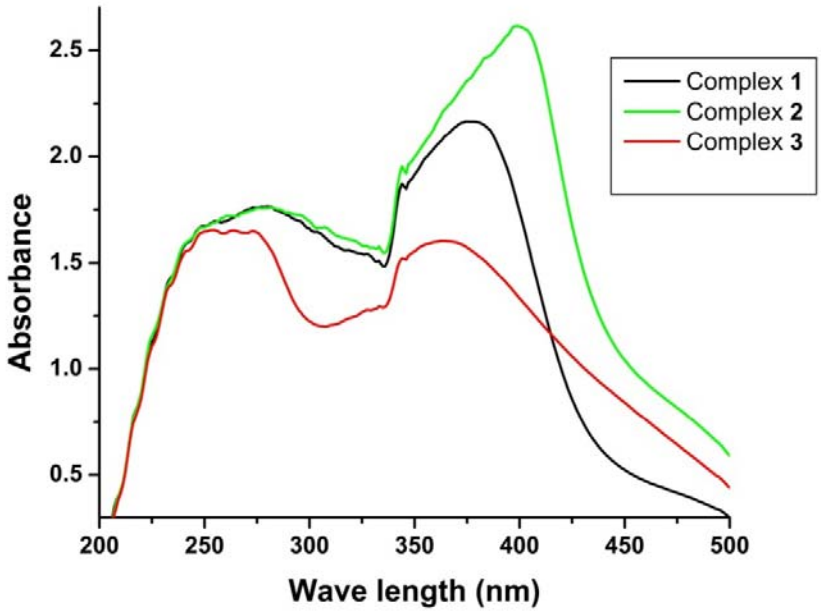

Fig. S6B UV-Vis spectra of trinuclear complexes in acetonitrile solution (charge transfer band).

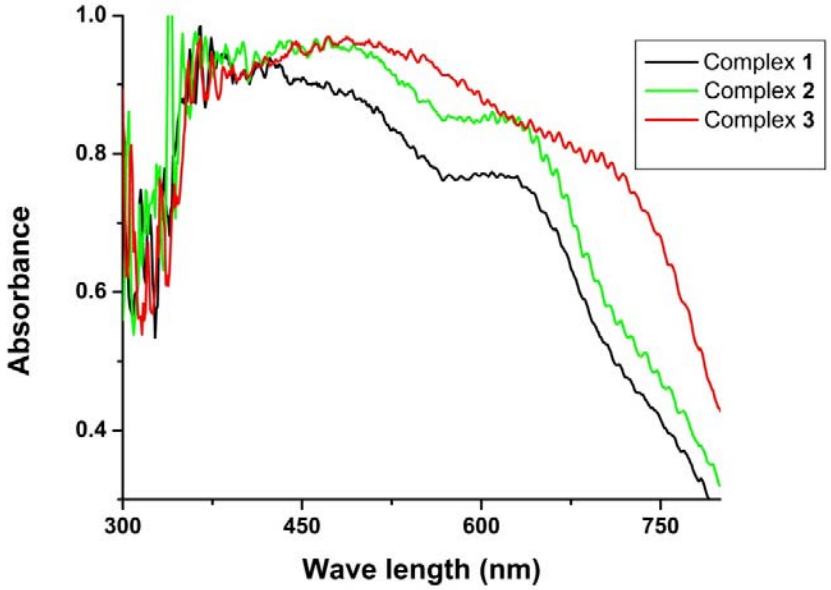

Fig. S7 UV-Vis spectra of trinuclear complexes in solid state

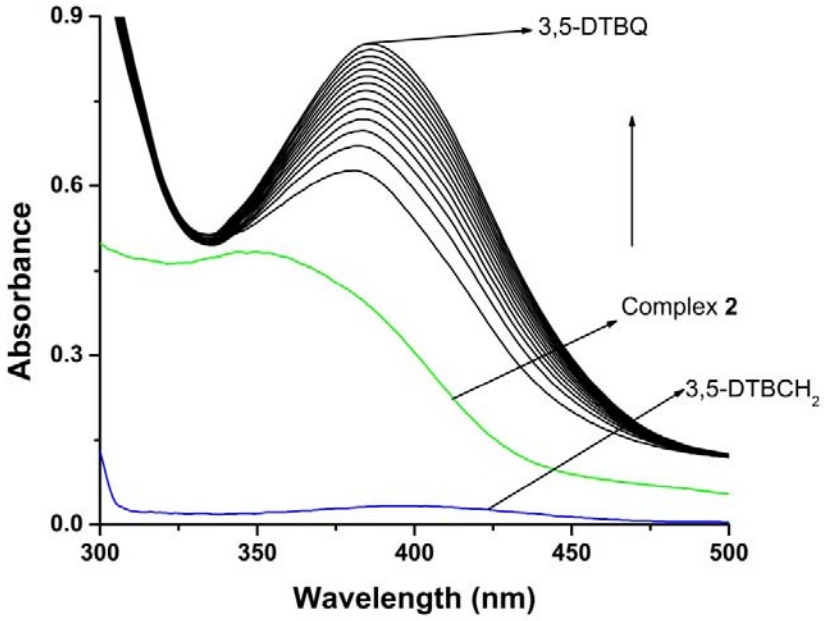

Fig. S8 Increase of the quinone band at around 400 nm after the addition of 100 equiv of 3,5-DTBC to an acetonitrile solution of complex **2**. The spectra were recorded at 5 min intervals.

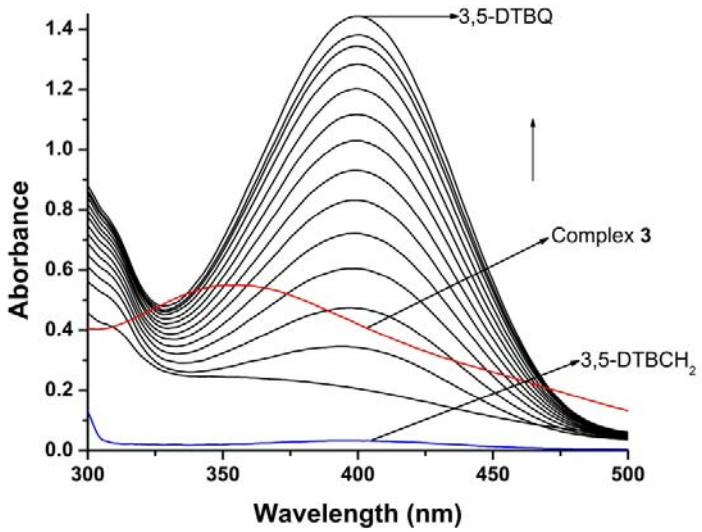

Fig. S9 Increase of the quinone band at around 400 nm after the addition of 100 equiv of 3,5-DTBC to an acetonitrile solution of complex **3**. The spectra were recorded at 5 min intervals.

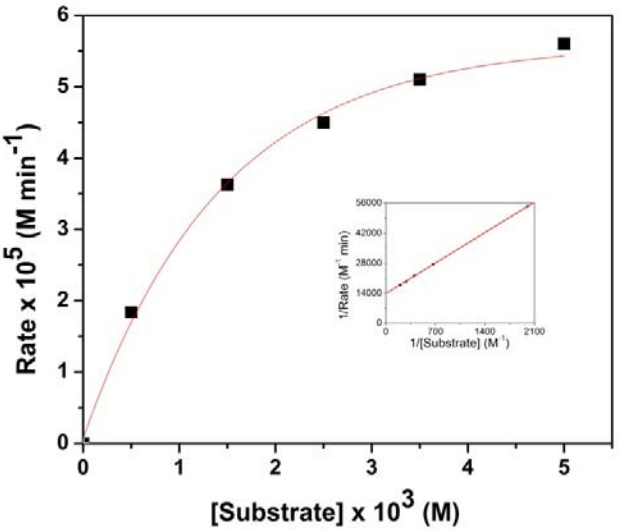

Fig. S10 Plot of the rate vs substrate concentration for complex **2**. Inset shows the corresponding Lineweaver−Burk plot.

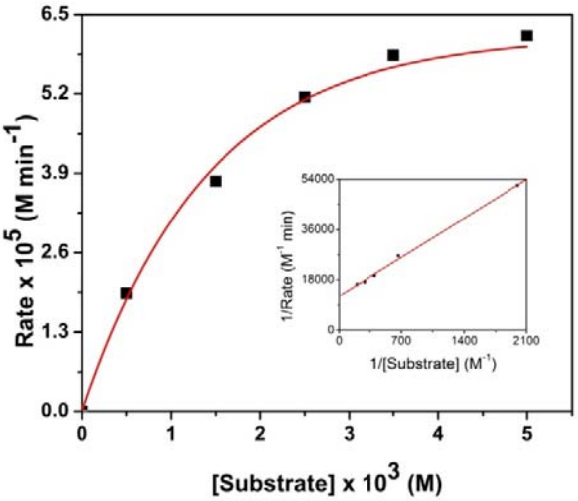

Fig. S11 Plot of the rate vs substrate concentration for complex **3**. Inset shows the corresponding Lineweaver−Burk plot.

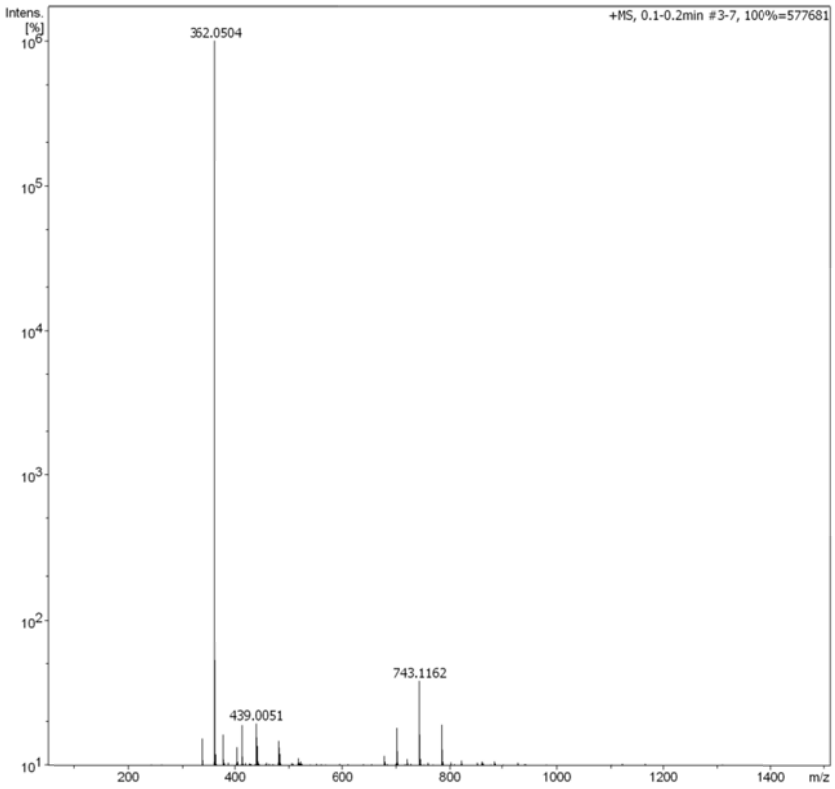

Fig. S12A Electrospray mass spectrum (ESI-MS positive) of complex **1** in acetonitrile solvent.

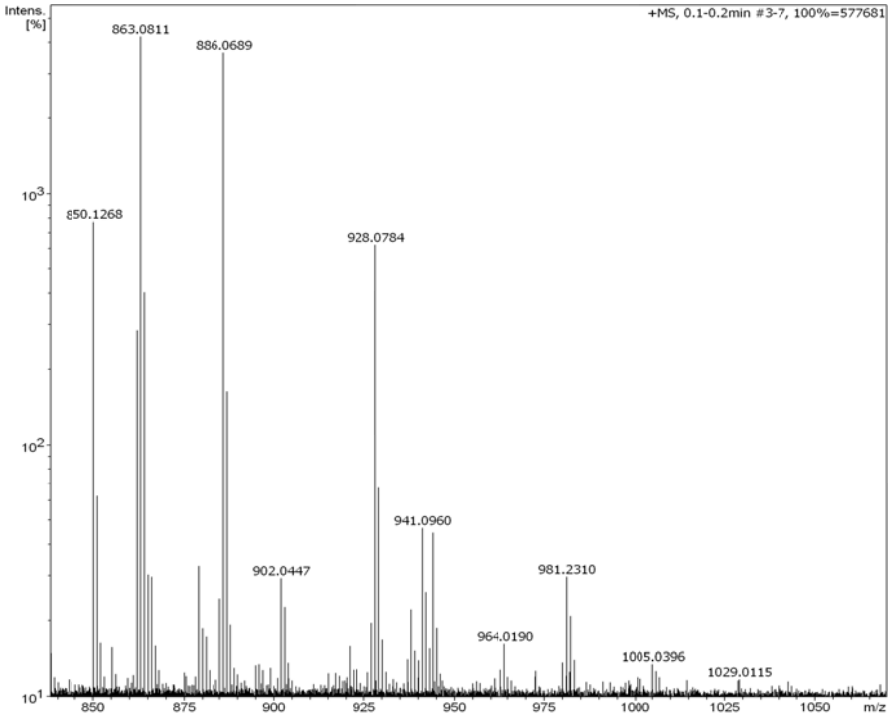

Fig. S12B Electrospray mass spectrum (ESI-MS positive) of complex **1** in acetonitrile solvent at higher m/z (expanded).

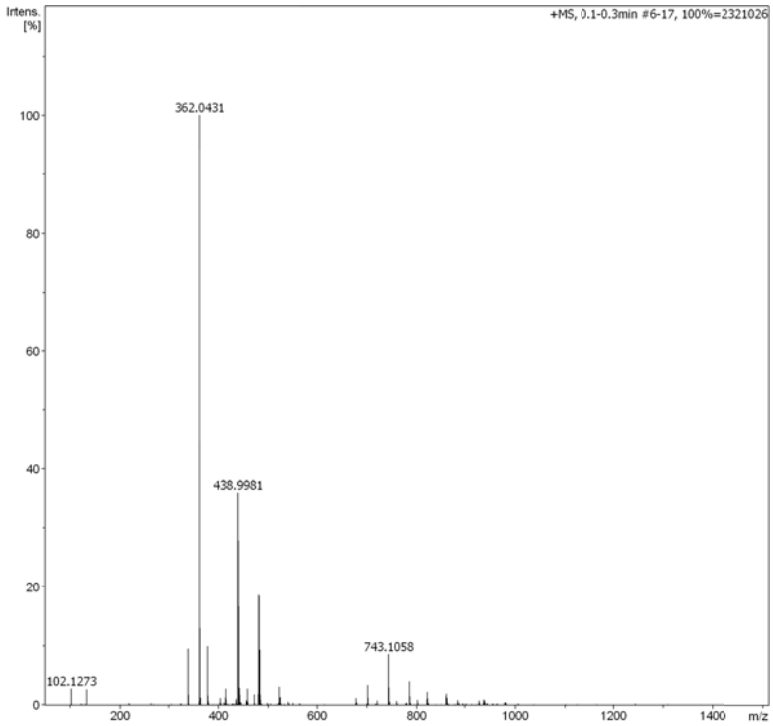

Fig. S13A Electrospray mass spectrum (ESI-MS positive) of complex **2** in acetonitrile solvent.

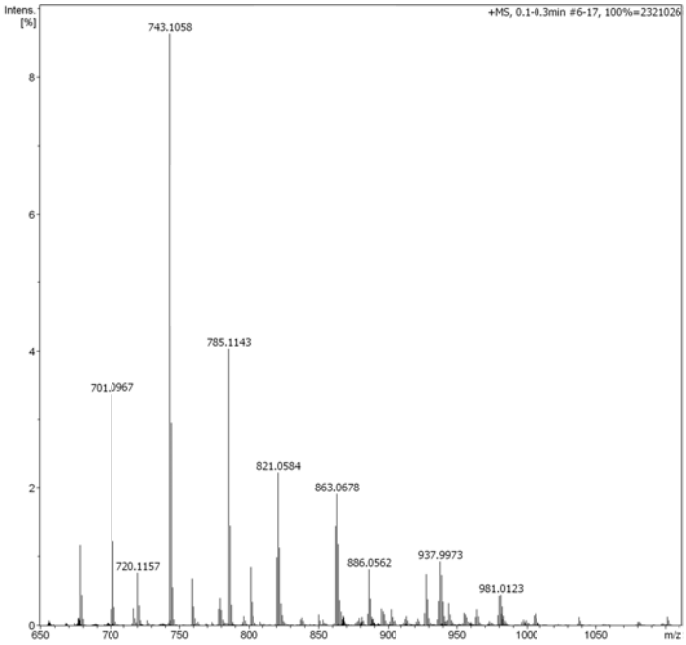

Fig. S13B Electrospray mass spectrum (ESI-MS positive) of complex **2** in acetonitrile solvent at higher m/z (expanded).

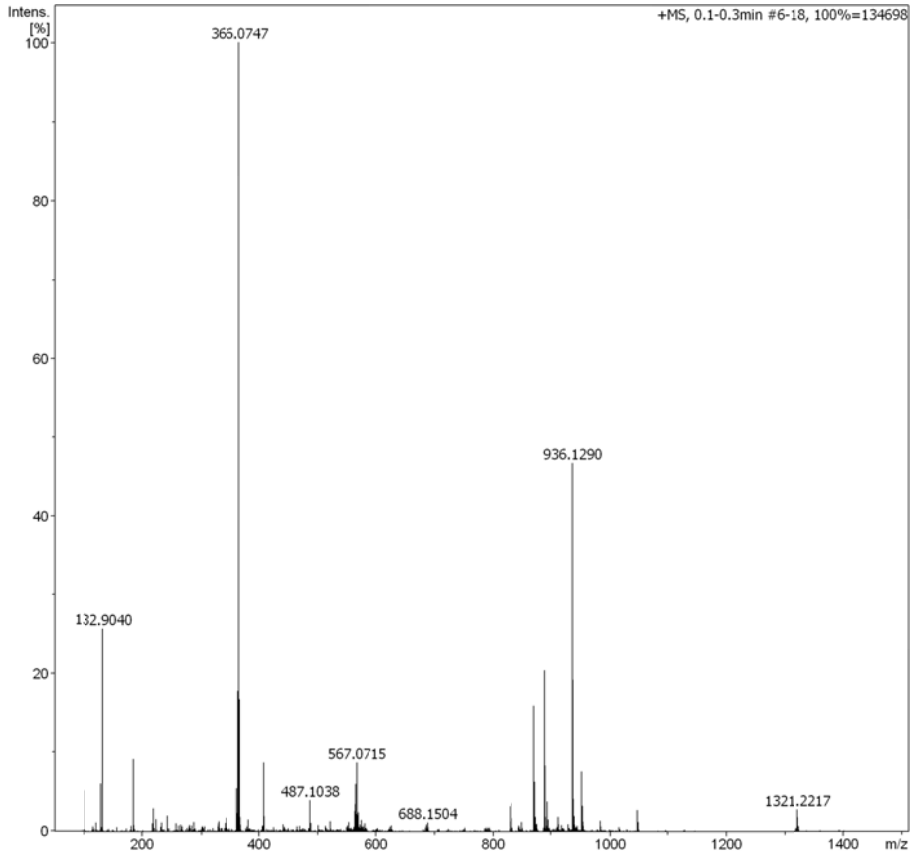

Fig. S14A Electrospray mass spectrum (ESI-MS positive) of complex **3** in acetonitrile solvent.

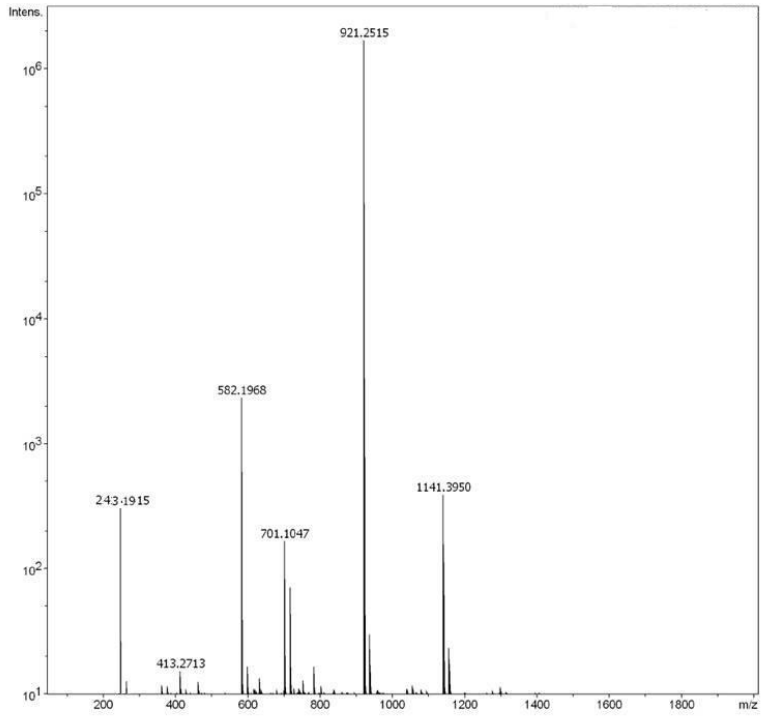

Fig. S15 Electrospray mass spectrum (ESI-MS positive) of complex **1** in acetonitrile solvent after addition of 3,5-DTBC.

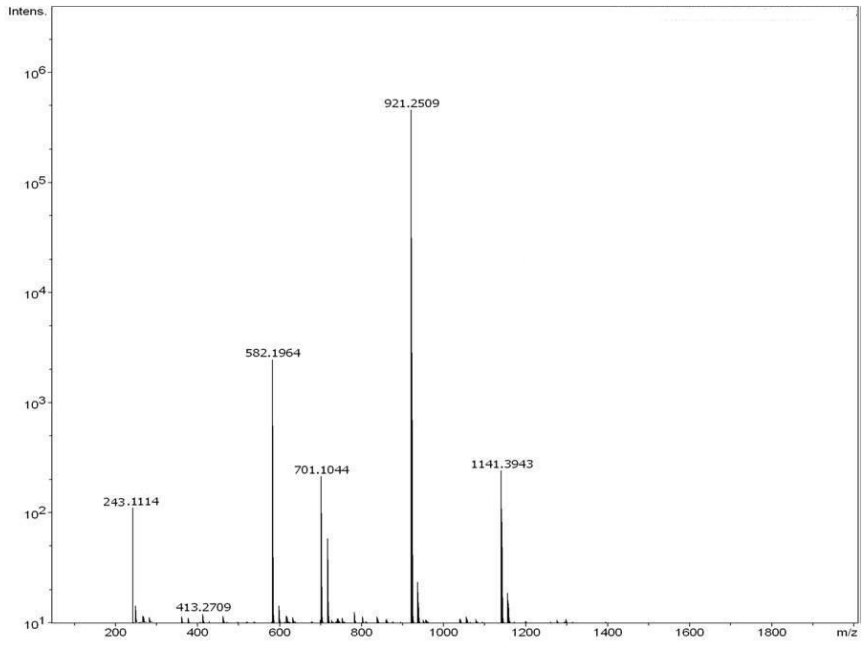

Fig. S16 Electrospray mass spectrum (ESI-MS positive) of complex **2** in acetonitrile solvent after addition of 3,5-DTBC.

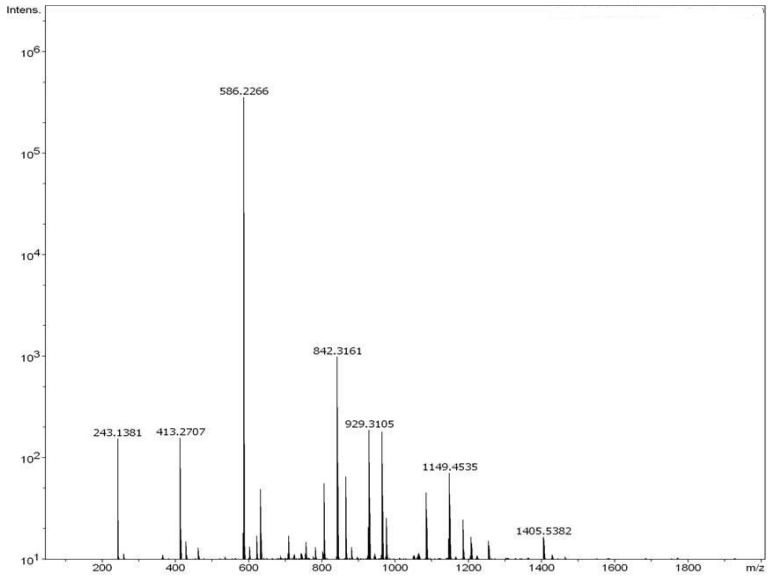

Fig. S17 Electrospray mass spectrum (ESI-MS positive) of complex **3** in acetonitrile solvent after addition of 3,5-DTBC.